

# Joint lensing–dynamics constraint on the elliptical galaxy mass profile from the largest galaxy–galaxy lens sample

Chin Yi Tan<sup>1,2</sup>  and Anowar Shajib<sup>3,2</sup> 

<sup>1</sup>Department of Physics, University of Chicago, Chicago, IL 60637, USA.  
email: [chinyi@uchicago.edu](mailto:chinyi@uchicago.edu)

<sup>2</sup>Kavli Institute for Cosmological Physics, University of Chicago, Chicago, IL 60637, USA

<sup>3</sup>Department of Astronomy & Astrophysics, The University of Chicago, Chicago, IL 60637, USA

**Abstract.** From various lensing and non-lensing observations, the total density profile in elliptical galaxies is well approximated by a power law mass distribution. However, as neither the dark matter nor the baryons individually follow the power law, this observational result has been referred to as the “bulge–halo conspiracy”. We investigate the consistency of this conspiracy with higher precision than previous studies with the largest ever sample of galaxy–galaxy lenses assembled from archival *Hubble Space Telescope* (*HST*) data. By performing lens modelling with power law profiles and combining them with stellar dynamics using the mass-sheet transformation, we can constrain the profile’s deviation from the power law model over a redshift range of 0.1 to 0.8. To uniformly model such a large sample of lens models, we use the automated modelling pipeline DOLPHIN. We also investigate the evolutionary trend of the total mass density slope of the lensing galaxies.

**Keywords.** gravitational lensing, galaxies: elliptical and lenticular, cD

## 1. Introduction

A galaxy-scale lens system is a lens configuration where a foreground (lensing) galaxy’s mass causes the background (source) galaxy’s light to be imaged into multiple lensed arcs or an Einstein ring. When the background galaxy of a galaxy-scale lens system does not contain a point source, we refer to the system as a galaxy–galaxy lens (as opposed to quasar lenses). As the lensed image is sensitive to the mass profile of the foreground galaxy, strong lensing at the galaxy scale can be used as a direct probe of the galaxies’ mass distribution. For an overview of the many applications of galaxy–galaxy lenses in astrophysics and cosmology, see [Shajib \*et al.\* \(2022\)](#).

Both strong lensing and non-lensing observations of elliptical galaxies have found that a power law profile,  $\rho(r) \propto r^{-\gamma}$ , can be used as a good model for the total density profile of the galaxies, with the slope of the power law being observed to be slightly steeper than isothermal ( $\gamma \sim 2.1$ ). This trend has been seen in observations using combinations of strong lensing, weak lensing, stellar dynamics, and X-ray observation ([Treu \*et al.\* \(2006\)](#), [Cappellari \*et al.\* \(2015\)](#), [Humphrey \*et al.\* \(2010\)](#), [Gavazzi \*et al.\* \(2007\)](#)). However, the individual dark matter and baryonic components of elliptical galaxies are not modelled with a power law, leading to the “bulge–halo conspiracy”. Simulation of galaxy formation has suggested that the power law-like nature of the total density profile can

be explained through the redistribution of the mass distribution of the galaxy through collisionless accretion in gas-poor mergers (Remus *et al.* (2013)).

From  $N$ -body cosmological simulations, it is found that elliptical galaxies are formed from hierarchical mergers of dark matter haloes that also contain stars and gas. The types of merger processes experienced by the elliptical galaxies can be inferred through observations of the evolution of the total density profile of the galaxies. If the elliptical galaxies formed through dissipative processes via “wet” gas-rich mergers, the dark matter halo will contract, and we would expect the total density slope to steepen with decreasing redshift. However, suppose galaxies are formed through dissipation-less gas-poor mergers. In that case, we expect the opposite trend with the dark matter halo expanding and the total density slope shallowing with decreasing redshift.

Analyses based on strong lensing and stellar dynamics have measured a slightly steepening trend in the total density slope with decreasing redshift consistent with gas-rich mergers (Sonnenfeld *et al.* (2013), Bolton *et al.* (2012)). In comparison, cosmological simulations such as Illustris and Magneticum have found either a constant mass density slope or a slightly shallowing slope with decreasing redshift (Xu *et al.* (2017), Remus *et al.* (2017)). Remus *et al.* (2017) have found that this apparent disagreement disappears when we apply the same joint lensing and dynamics analysis to the simulated galaxies, which might indicate that systematic errors are present in the joint lensing and dynamics analysis.

Therefore, we assembled one of the largest uniformly modelled lens samples to investigate the above mentioned tensions. In Section 2, we first discuss the improvements made in our lens modelling pipeline compared to previous joint lensing and dynamics analysis. We then used our lens models to investigate the redshift trend of the total mass density slope of elliptical in Section 3. Finally, in Section 4, we combine our lens models with kinematic data to measure any deviation of our total density profiles with the power law.

## 2. Uniform Lens modelling

In many previous joint lensing and dynamics analyses, the lens image is first modelled with a singular isothermal ellipsoid (SIE) profile to obtain the Einstein radius. The mass density slope is then measured using kinematic data, assuming a power law model. However, using *HST*-quality imaging data, it is also possible to constrain the total density slope directly from images. Therefore, if we model *HST* images with the more flexible power-law ellipsoidal mass distribution (PEMD) model, we can extract all the information present in the lensed arcs. This also allows us to use the additional kinematic data to fit profiles beyond the power law.

We present Project Dinos, which aims to study the evolution in the properties of elliptical galaxies by remodelling archival *HST* images of the galaxy–galaxy lens systems with the more flexible PEMD model. Our lens samples comprised of a subset of lens systems from various surveys such as the Sloan Lens ACS (SLACS) survey, the Strong Lensing Legacy Survey (SL2S), and the BOSS Emission-Line Lens Survey (BELLS) based on the availability of visible-band *HST* imaging. To uniformly model such a large lens sample, we use the lens modelling pipeline DOLPHIN (Shajib *et al.* (2021)), which employs the lens modelling software LENSTRONOMY (Birrer *et al.* (2018), Birrer *et al.* (2021)) as its modelling engine. Whereas LENSTRONOMY contains many features to allow the user to fine-tune their lens models, DOLPHIN uses a semi-automated decision-making process and has a simplified user interface to reduce the time and effort needed for the user to model a lens system.

For the lensing galaxy, we set the mass profile to be the power-law ellipsoidal mass distribution (PEMD) while using two elliptical Sérsic profiles for the light profile. We then

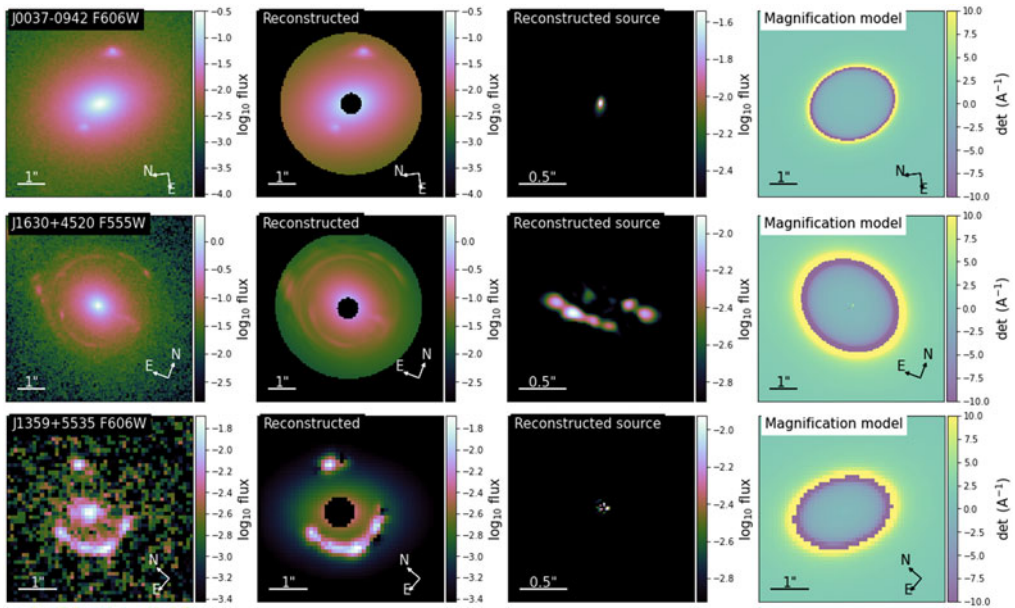


**Figure 1.** DOLPHIN lens models for selected SLACS (first two rows) and SL2S (last row) lenses. The first column shows *HST* images of the lenses in the visible band. The label in the first column indicates the name of the lens and band of the image. The second column shows the model’s reconstructed image of the system, while the reconstructed source is shown in the third column. The lens model magnification map is shown in the fourth column.

use a combination of elliptical Sérsic profile and a basis set containing multiple shapelet components (Birrer *et al.* (2015)) to recreate the light profile of the source galaxy.

We use the Markov chain Monte Carlo (MCMC) method using EMCEE to obtain the posterior probability distribution function of the model parameters. Figure 1 shows examples of lens models from the SLACS and SL2S samples successfully modelled by DOLPHIN. A number of lens systems contain complicated lens features and they are not successfully reconstructed by the modelling pipeline. These lenses must be modelled on a case-by-case basis and thus are excluded from our analysis. Out of the initial 103 lens systems of SLACS, SL2S and BELLS lenses, we successfully model 77 systems.

### 3. The evolution of the total density slope

Before we combine our lens models with kinematic data, we first probe the evolution of the lensing galaxy’s power-law mass density slope obtained from lensing-only information. Figure 2 shows the individual power-law mass density slope,  $\gamma_{\text{PL}}$ , for each lens system plotted against the redshift their lensing galaxy. We fit a linear relation for the power-law mass density slope as a function of the redshift of the lensing galaxy,  $z$ , and the ratio of the effective radius of the galaxy’s light profile to its Einstein radius,  $R_{\text{eff}}/\theta_{\text{E}}$ . In addition, we also allow for the linear fit to contain a redshift-independent intrinsic scatter  $\sigma_{\gamma}$ . The median power-law mass density slope for the combined population is measured to be

$$\langle \gamma_{\text{PL}}(z) \rangle = (2.06 \pm 0.04) + (0.29 \pm 0.19)(z - 0.3) + (0.03 \pm 0.05) \left( \frac{R_{\text{eff}}}{\theta_{\text{E}}} - 1 \right), \quad (1)$$

and the intrinsic scatter of power-law mass density slope is  $\sigma_{\gamma} = 0.11 \pm 0.01$ . Therefore, we found that the total mass density slope shallows with decreasing redshift at a significance of  $1.5\sigma$ . This is opposite to the trend with previous joint lensing and dynamics analyses (Sonnenfeld *et al.* (2013), Bolton *et al.* (2012)) but consistent with comological simulation.

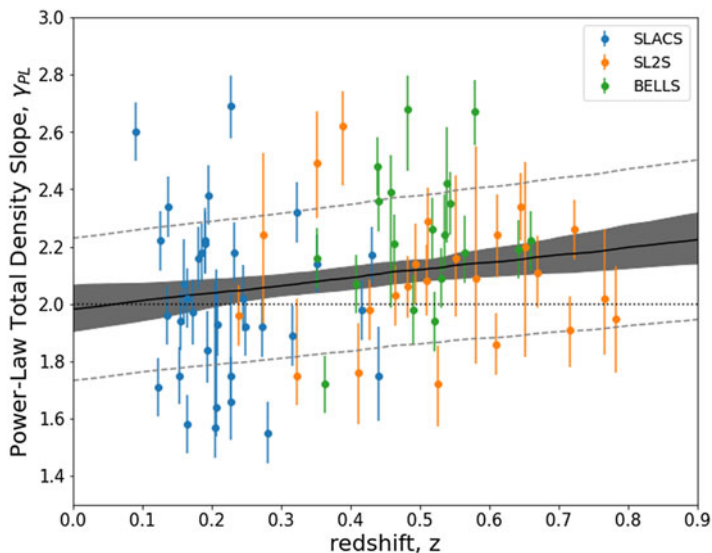


**Figure 2.** The evolution of the power-law mass density slope,  $\gamma_{\text{PL}}$ , over the redshift of the lensing galaxy,  $z$ . The coloured points represent the measurement and uncertainty of  $\gamma_{\text{PL}}$  for each individual lens system obtained from DOLPHIN. The whole black line traces the median fit for  $\langle \gamma_{\text{PL}} \rangle$ , while the grey shaded regions represent the  $1\sigma$  credible region both marginalised over the  $R_{\text{eff}}/\theta_{\text{E}}$  dependence. The intrinsic scatter,  $\sigma_{\gamma}$ , is represented by the dashed lines.

However, due to the large intrinsic scatter found in the fits, a larger lens model sample is needed to increase the statistical power of the analysis.

#### 4. Measuring the deviation from power-law with the mass-sheet transform

The mass-sheet transform (MST) (Falco *et al.* (1985)) is a transformation that changes the shape of the lensing galaxy’s profile while preserving all its lensing observables. Under the MST, the convergence field of the lensing galaxy,  $\kappa$ , transforms as,

$$\kappa \rightarrow \kappa' = \lambda_{\text{int}}\kappa + (1 - \lambda_{\text{int}}), \quad (2)$$

where  $\lambda_{\text{int}}$  is the internal MST parameter for the transformation. For velocity dispersion measurements obtained from a single aperture, the velocity dispersion approximately scales with the internal MST parameter (Birrer *et al.* (2020)) as

$$\sigma \rightarrow \sqrt{\lambda_{\text{int}}}\sigma. \quad (3)$$

Therefore, by comparing velocity dispersion predicted by our power-law-based lens models to the measured dispersion from spectroscopy, we can measure the MST parameter,  $\lambda_{\text{int}}$ , and thus probe the deviation from the power law.

We use the hierarchical strong lensing systems analysis pipeline HIERARC (Birrer *et al.* (2020)) to provide a population-level estimate of  $\lambda_{\text{int}}$ . We also incorporate the external convergence measurements,  $\kappa_{\text{ext}}$ , from the line-of-sight galaxies and stellar anisotropy of the lensing galaxy using the Osipkov-Merritt formalism in our analysis. Similar to the evolution of the power-law mass density slope, we fit a linear relation for  $\lambda_{\text{int}}$  as a function of the redshift of the lensing galaxy,  $z$ , and the ratio of the effective radius of the galaxy’s light profile to its Einstein radius,  $R_{\text{eff}}/\theta_{\text{E}}$ , in the form of

$$\langle \lambda_{\text{int}} \rangle = \lambda_{\text{int}}^{\text{ref}} + \alpha_{\lambda}(z - 0.3) + \beta_{\lambda}\left(\frac{R_{\text{eff}}}{\theta_{\text{E}}} - 1\right). \quad (4)$$

Tan *et al.* (in prep) will present the values of the associated parameters and provide discussion on its implication for the evidence of the deviation of the total mass profile from the power law. In the near future, we intend to extend our analysis to a composite model consisting of both dark matter and baryonic components using techniques similar to those employed by Shajib *et al.* (2021) to obtain a more physically motivated mass profile of elliptical galaxies beyond the power law.

## 5. Acknowledgements

This project and a portion CYT's travel to the symposium were supported by NASA through the NASA Hubble Fellowship grant HST-HF2-51492 awarded to AJS by the Space Telescope Science Institute, which is operated by the Association of Universities for Research in Astronomy, Inc., for NASA, under contract NAS5-26555. Another portion of CYT's travel cost was supported by the Department of Energy grant DE-AC02-07CH11359 subcontract 6749003 at Fermilab and the University of Chicago.

## References

- Birrer S., Amara A., Refregier A. 2015, *ApJ*, 813, 102  
Birrer S., Amara A. 2018, *Physics of the Dark Universe*, 22, 189  
Birrer S., et al. 2020, *A&A*, 643, A165  
Birrer S., et al. 2020, *JOSS*, 6, 3283  
Bolton A., et al. 2012, *ApJ*, 757, 82  
Cappellari M., et al. 2015, *ApJ*, 804, L21  
Falco E. E., Gorenstein M. V., Shapiro I. I. 2015, *ApJ*, 289, L1  
Gavazzi R., et al. 2007, *ApJ*, 667, 176  
Humphrey P. J., Buote D. A. 2010, *MNRAS*, 403, 2143  
Remus R.-S., et al. 2013, *ApJ*, 766(2), 71  
Remus R.-S., et al. 2017, *MNRAS*, 464(3), 3742–3756  
Shajib A. J., et al. 2022, arXiv e-prints, p. arXiv:2210.10790  
Shajib A.J., Treu T., Birrer S., Sonnenfeld A., 2021, *MNRAS*, 503(2), 2380–2405  
Sonnenfeld A., et al. 2013, *ApJ*, 777(2), 98  
Treu T., Koopmans L. V., Bolton A. S., Burles S., Moustakas L. A., 2006, *ApJ*, 640, 662  
Xu, D., et al. 2017, *MNRAS*, 469(2), 1824–1848